Ocean Dynamics (2016) 66:659–669
DOI 10.1007/s10236-016-0948-9

On the effect of sea spray on the aerodynamic surface drag under severe winds

Yuliya Troitskaya[1,2] · **Ekaterina Ezhova**[1,2] · **Irina Soustova**[1,2] · **Sergej Zilitinkevich**[2,3,4,5,6]

Received: 26 August 2015 / Accepted: 9 March 2016 / Published online: 19 March 2016

Abstract We investigate the effect of the sea spray on the air-sea momentum exchange during the entire "life cycle" of a droplet, torn off the crest of a steep surface wave, and its fall down to the water, in the framework of a model covering the following aspects of the phenomenon: (1) motion of heavy particle in the driving air flow (equations of motion); (2) structure of the wind field (wind velocity, wave-induced disturbances, turbulent fluctuations); (3) generation of the sea spray; and (4) statistics of droplets (size distribution, wind speed dependence). It is demonstrated that the sea spray in strong winds leads to an increase in the surface drag up to 40 % on the assumption that the velocity profile is neutral.

Keywords Spray · Wind · Surface waves · Surface drag

Responsible Editor: Jörg-Olaf Wolff

Yuliya Troitskaya and Ekaterina Ezhova contributed equally to this work.

✉ Ekaterina Ezhova
ezhova@hydro.appl.sci-nnov.ru

Yuliya Troitskaya
yuliya@hydro.appl.sci-nnov.ru

Irina Soustova
soustova@hydro.appl.sci-nnov.ru

Sergej Zilitinkevich
sergej.zilitinkevich@fmi.fi

[1] Institute of Applied Physics Russian Academy of Sciences, 46 Ul'yanov str., 603950 Nizhny Novgorod, Russia

[2] Department of Radiophysics, Lobachevsky State University of Nizhni Novgorod, 23 Gagarin avenue, 603950 Nizhny Novgorod, Russia

[3] Finnish Meteorological Institute, PO Box 503, 00101 Helsinki, Finland

[4] Division of Atmospheric Sciences, University of Helsinki, PO Box 48, 00014 Helsinki, Finland

[5] Faculty of Geography, Lomonosov Moscow State University, GSP-1, Leninskie Gory, 119991 Moscow, Russia

[6] Institute of Geography, Russian Academy of Sciences, 29 Staromonetniy pereulok, 119017 Moscow, Russia

1 Introduction

Anomalously low aerodynamic roughness of the sea surface at hurricane wind speeds exceeding 30–35 m/s has been observed recently in a number of field and laboratory measurements (Powell et al. 2003; Donelan et al. 2004; Jarosz et al. 2007; Troitskaya et al. 2011). The first evidence has been found in the pioneering experiment of Powell et al. (2003) aimed to measure wind velocity profiles in the marine atmospheric boundary layer (MABL) in tropical cyclones. The similar effect of water surface drag's "crisis" has been detected in indirect measurements of currents, induced by tropical cyclones in the coastal zone (Jarosz et al. 2007). Both experiments have shown that the drag coefficient,

$$C_D = \frac{u_*^2}{U_{10}^2}, \tag{1}$$

(u_* is the wind friction velocity, U_{10} is the wind speed at the standard height $H_{10}=10$ m) first grows with the wind speed, reaches its maximum near $U_{10}=30$–35 m/s, and then decreases.

In the laboratory experiments (Donelan et al. 2004), the similar saturation of drag coefficient C_D at $U_{10}>33$ m/s was observed, and in (Troitskaya et al. 2011), the similar tendency to saturation of C_D for $U_{10}>25$ m/s was found. Both experiments demonstrated significantly lower values of C_D than

those given by Charnock formula extrapolated to hurricane winds. Recent re-analysis of the experimental data in the papers by Foreman and Emeis (2010) and Andreas et al. (2012) and a model of the air-sea interface by Bye et al. (2010, 2014) confirmed a tendency to saturation of the surface drag coefficient at high winds qualitatively explained by geometric similarity of surface waves maintained at strong winds. Comparing experimental data in (Troitskaya et al. 2011) with predictions of the theoretical model of a turbulent boundary layer over a wavy water surface (Troitskaya and Reutov 1995; Troitskaya and Rybushkina 2008) demonstrates reasonable agreement when the theory accounts for the high-frequency part of the wind-wave spectrum.

Note, however, that the theoretical model proposed in (Troitskaya and Reutov 1995; Troitskaya and Rybushkina 2008) does not take into account the rheology of the atmospheric boundary layer at hurricane winds due to the presence of sea sprays. The influence of sea spray on the surface drag in the atmospheric boundary layer has been estimated recently by Kudryavtsev and Makin (2011). Two physical mechanisms responsible for the deformation of the velocity profile in MABL and hence aerodynamic drag change have been considered. The first one is the stable stratification in the air flow due to levitating sprays (Makin 2005; Kudryavtsev 2006). The second one is the direct spray effect on the momentum exchange (Andreas 2004; Kudryavtsev and Makin 2011). According to Makin (2005), Kudryavtsev (2006), concentration of levitating sprays in the turbulent air flow decays with the distance from the surface. This results in the stable density stratification of the two-phase, air-spray medium. Suppression of the vortex motion in the turbulent stably stratified boundary layer leads to weakening of turbulent exchange, i.e., to decreasing of the tangential turbulent stress in the boundary layer and, according to Eq. (1), reduction of the drag coefficient. This mechanism has been investigated in detail by Andreas et al. (1995) for the case of the heavy levitating droplets. However, the estimates of Kudryavtsev (2006) have demonstrated that for the spray concentration measured in MABL (Andreas 1998), this mechanism provides a reduction of C_D by only 0.1 % for a wind speed of about 50 m/s. Noticeable reduction of C_D has been observed only when the spray concentration has been increased artificially by three orders of magnitude as compared to the experimental data (Andreas 1998). To explain the observed effect, a volume spray source located at the distance of a significant wave height from the water surface has been introduced by Kudryavtsev (2006) to model the droplets injected from the crests of the steep waves. Within the hypothesis of the high concentration of levitating spray created by this source, a considerable reduction of the drag coefficient has been obtained (Kudryavtsev 2006). A hypothesis of the volume spray source presumes the injection of droplets in the air flow at a wind speed similar to a jet from a sprayer. The effect of stratification due to spray has also been considered by Bye and Jenkins (2006). They employ Monin-Obukhov theory for stratified boundary layers and get a modified wind velocity profile in the presence of spray droplets suspended in the air. This model also uses the estimates of bulk velocity of spray injection and the result depends significantly on this velocity. The wide maximum of the drag coefficient is obtained within the model, however, at somewhat higher velocities as compared to the experimental data. These results are in qualitative agreement with the theoretical predictions in terms of the inertially coupled system of Bye et al. (2010, 2014). The model uses several constants obtained from the approximation of the experimental data and involves spray effect for the explanation of the low friction at high winds.

Another option of the spray impact on the wind velocity profile is a direct momentum exchange between spray and the air flow (Andreas 2004; Kudryavtsev and Makin 2011). In this case, the mechanism of the droplets' formation is of importance. According to Andreas et al. (1995) and Andreas (1998), three types of droplets can be specified: film, jet, and spume droplets. Film and jet droplets appear from the bubbles bursting on the surface. A bubble film degrades to form hundreds of film droplets sized 0.5–5 μm. Bubble burst produces a jet which in its turn is a source of several jet droplets, sized 3–50 μm depending on the bubble diameter. Spume droplets are formed as a result of the wind tearing spume off the wave crests. Spume droplets are the largest ones with a minimum size of 20 μm. Under strong and hurricane winds, jet and spume droplets are the most important for momentum exchange with the air flow. Torn from the water surface, a droplet is entrained by the air flow whose velocity often far exceeds its initial velocity. Thus, it might be expected that the momentum would be taken from the air flow by droplets which should lead to an increase of the surface drag. The reverse process is also possible when the large droplets accelerated in the air flow to high speeds, fell on the surface, and adjusted to the low air velocities near the surface deliver momentum to the wind. When the latter effect dominates, the air flow accelerates and the drag coefficient reduces. This mechanism has been considered by Kudryavtsev and Makin (2011) within a semi-empirical model. An important element of the model proposed in (Kudryavtsev and Makin 2011) similar to (Kudryavtsev 2006) is a volume source of droplets whose parameters determine the effectiveness of the momentum exchange. The determining hypothesis assumes that the droplets get to the air flow at the height of crests of dominant surface waves having a speed equal to the wind speed. Obviously, this assumption misses an important part of the "life cycle" of spray during which droplets accelerate from the velocity they had at the water surface to the wind speed.

The purpose of the paper is to calculate the effect of inertia of droplets on neutral surface drag coefficient (or roughness height), which is not affected by stratification of the boundary layer. The effect of stratification can be then taken into account

independently basing on the Monin-Obukhov similarity theory (see Bye and Jenkins 2006 and Bao et al. 2011). In the present work, we consider the momentum exchange of the air flow with sea spray during the complete life cycle of the droplet, torn off the crest of a steep surface wave, and then falling down to the water. The model includes the following constituents: a model of motion of a heavy particle in the forcing air flow (equations of motion); a model of the wind flow (wind velocity, wave-induced disturbances, turbulent fluctuations); a model of spray injection; and the statistics of droplets (size distribution, wind speed dependence). We employ the Lagrangian stochastic model where the interaction of the droplets with the turbulent fluctuations in the air flow has been modeled in terms of the Markovian chain similar to Edson and Fairall (1994). For modeling turbulent air flow, we account only for the vertical velocity fluctuations. In estimations of the initial velocities of the droplets at the water surface, we used the recent field data on the statistics of white caps from (Kleiss and Melville 2010).

2 The resistance law in MABL at strong winds in presence of spray

We will first derive the resistance law of the sea surface taking into account the momentum flux associated with spray. The effect of spray on the air flow can be described by bulk force. To calculate the density of this force, we consider a simplified model of the two-dimensional waves on the water surface (the problem, however, can be easily generalized to the three-dimensional case) and use a wave following curvilinear reference frame defined by the mapping:

$$x = x^*, \tag{2}$$

$$z = z^* + \eta(x^*, t^*), \tag{3}$$

$$t = t^*, \tag{4}$$

$\eta(x^*, t^*)$ is a vertical displacement of the water surface due to the wave. In this reference frame, a horizontal projection of the Reynolds equation yields

$$\rho_a\left(\frac{\partial\langle u\rangle}{\partial t^*}-\frac{\partial\langle u\rangle}{\partial z^*}\frac{\partial\eta}{\partial t^*}+\langle u\rangle\left(\frac{\partial\langle u\rangle}{\partial x^*}-\frac{\partial\langle u\rangle}{\partial z^*}\frac{\partial\eta}{\partial x^*}\right)+\langle v\rangle\frac{\partial\langle u\rangle}{\partial z^*}\right)+ +\frac{\partial\langle p\rangle}{\partial x^*}-\frac{\partial\langle p\rangle}{\partial z^*}\frac{\partial\eta}{\partial x^*}=\rho_a\left(\frac{\partial\sigma_{xx}}{\partial x^*}-\frac{\partial\sigma_{xx}}{\partial z^*}\frac{\partial\eta}{\partial x^*}+\frac{\partial\sigma_{xz}}{\partial z^*}\right)+f, \tag{5}$$

and the continuity equation is

$$\frac{\partial\langle u\rangle}{\partial x^*}-\frac{\partial\langle u\rangle}{\partial z^*}\frac{\partial\eta}{\partial x^*}+\frac{\partial\langle v\rangle}{\partial z^*}=0. \tag{6}$$

In Eqs. (5) and (6), u is a horizontal velocity, ν is a vertical velocity, $\sigma_{xx,\ xz}$ are Reynolds stresses, ρ_a is an air density, p is pressure, and f is a horizontal projection of the density of the bulk force due to the momentum exchange with spray, i.e., momentum transferred from the droplets to the air flow per unit volume per unit time. The designation $< \ldots >$ corresponds to statistical averaging over the ensemble of turbulent pulsations.

In stationary conditions, averaging of Eq. (5) over x^* (see Appendix) and integration over z^* yields the following expression for the conservation of momentum flux:

$$\rho_a\,\overline{\sigma_{xz}}^{x^*}=\rho_a u_*^2-\rho_a\tau_{\mathrm{wave}}(z^*)-F(z^*), \tag{7}$$

where we take into account the boundary condition $\sigma_{xz}{}^{x^*}\to u_*^2$ when $z^*\to\infty$. Here, $\tau_{\mathrm{wave}}(z^*)$ is a wave momentum flux caused by the form drag of the water surface (a function of z^* decreasing with the distance from the surface),

$$F(z^*)=-\int_{z^*}^{\infty}\bar{f}^{x^*}(z')dz' \tag{8}$$

is momentum delivered from the air flow to spray in the layer from current z^* to infinity. If droplets are accelerated by the flow, then $F>0$; in the opposite case, $F<0$.

We use the Boussinesq approximation for the turbulent momentum flux: $\sigma_{xz}{}^{x^*}=K_m\frac{dU_0}{dz^*}$ (U_0 (z^*) is a horizontal component of the air flow velocity). For the eddy viscosity coefficient K_m, we adopt the empirical self-similar function obtained by Smol'yakov (1973) for the turbulent flow over a hydrodynamically smooth plate:

$$K_m(z^*)=\nu_a\left(1+\frac{\kappa u_* z^*}{\nu_a}\left(1-\exp\left\{-\left(\frac{u_* z^*}{\nu_a H}\right)^2\right\}\right)\right), \tag{9}$$

where $H=22.4$ and $\kappa=0.4$ is von Kármán constant.

Integrating Eq. (7) over z^* with account of Eq. (9) gives the velocity profile of the air flow in MABL:

$$U_0(z^*)=\int_0^{z^*}\frac{u_*^2-\tau_{\mathrm{wave}}(z')-F(z')/\rho_a}{K_m(z')}dz'. \tag{10}$$

Far from the surface, Eq. (10) tends to

$$U_0(z^*)=\frac{u_*}{\kappa}\ln\frac{z^*}{z_0}-u_{\mathrm{spray}}; \tag{11}$$

where z_0 is the surface roughness determined by the skin friction and form drag. $u_{\mathrm{spray}}(z^*)=\int_0^{z^*}\frac{F(z')/\rho_a}{K_m(z')}dz'$ is a modification of the air velocity profile due to the momentum exchange between the air flow and spray described by the force $F(z)$. In order to calculate function $F(z)$, it is necessary to

calculate the horizontal momentum gained by the droplet of the radius a when it moves in the air flow above z^*.

3 Motion of a heavy particle in the air flow

Momentum exchange of spray with the turbulent air flow in MABL is described within the Lagrangian stochastic model of turbulent transport developed by Edson and Fairall (1994). We consider a separate droplet and calculate the momentum delivered (or gained) by the droplet to the air flow during its "life cycle" from being injected to the air to dropping on the surface. The droplet is considered as a small sphere of radius a under the forcing of the viscous resistance and gravity, the interaction between the droplets is neglected:

$$\frac{4}{3}\pi\rho_p a^3\frac{d\vec{V}_p}{dt}=\frac{1}{2}\pi a^2\rho_a\beta\left(\vec{U}_0-\vec{V}_p\right)|\vec{V}_p-\vec{U}_0| + \frac{4}{3}\pi\rho_p a^3\vec{g}. \quad (12)$$

Here, $\vec{V}_p$ is a droplet velocity, ρ_p is its density, $\vec{U}_p$ is the air flow velocity, $\vec{g}$ is the acceleration due to gravity, $\beta=\frac{12}{Re}K$ is the drag coefficient of a spherical particle, where K is the dimensionless parameter equal to the ratio of the resistance force at the droplet to the Stokes force. We used the dependency of K on the Reynolds number from (Edson and Fairall 1994).

Suppose that the droplet velocity can be represented as a superposition:

$$V_{pi}=\overline{V}_{pi}+v_{pi}, \quad (13)$$

where $\overline{V}_{pi}$ is the average velocity and v_{pi} is the pulsating velocity due to the turbulent fluctuations in the air flow, i stands for x, y. The difference between our model and the model of Edson and Fairall (1994) is that the horizontal droplet velocity in our model is not equal to the wind speed. The droplet is injected from the water surface with its own velocity (discussed in Section 4), and then subsequently relaxes to the velocity of the ambient air flow. Note that the turbulent pulsations of the wind are accounted only in the vertical velocity. Horizontal pulsations are small compared to the average wind speed and in our model they are neglected.

The equation in finite differences for the horizontal velocity

$$U_p(t+\Delta t)=\left(1-\frac{K\Delta t}{T_R}\right)U_p(t)+\frac{K\Delta t}{T_R}U_0, \quad (14)$$

where $T_R=\frac{2}{9}\frac{\rho_p}{\rho_a}\frac{a^2}{\nu_a}$ is the relaxation time of Stokes sphere.

The equation for the vertical velocity:

$$W_p(t+\Delta t)=\left(1-\frac{\Delta t}{\tau_w^p}\right)W_p(t)+\sigma_w^p\left(\frac{2\Delta t}{\tau_w^p}\right)^{1/2}\zeta(t) + \frac{\Delta t}{\tau_w^p}\overline{W}_p. \quad (15)$$

here, τ_w^p is the droplet integral timescale, σ_w^p is the square root of the droplet vertical velocity variance, and $\zeta(t)$ is the δ-correlated random process with the Gaussian probability density function. The parameters σ_w^p and τ_w^p can be derived from the corresponding characteristics of the air flow turbulent pulsations σ_w and τ_L, specified by the following expressions based on experimental data (see Edson and Fairall (1994) and references therein):

$$\sigma_w=1.27u_*,\ \tau_L=0.24z/u_*. \quad (16)$$

4 A model of the air flow over the wavy water surface

The average wind velocity field in MABL is determined by the turbulent, wave, and spray momentum exchange. The turbulent momentum exchange was parameterized by the formula for the friction velocity u_* obtained by Foreman and Emeis (2010) on the base of the experimental data for $U_{10}>8$ m/s:

$$u_*=C_m(U_{10}-8)+0.27, \quad (17)$$

here, $C_m=0.051$, U_{10} and u_* have dimension [m/s]. Thus, accounting for the logarithmic profile of wind speed $U_{10}=\frac{u_*}{\kappa}\ln\frac{z_{10}}{z_0}$, we get for the roughness height:

$$z_0=z_{10}\exp\left(\frac{-\kappa(u_*+0.138)}{0.051u_*}\right). \quad (18)$$

According to this parameterization, the roughness height saturates at strong winds, opposite to classic Charnock formula $z_0=\frac{\alpha u_*^2}{g}$.

Modeling wave-induced wind disturbances, was based on the qualitative picture of the stormy sea. As can be seen from a typical photo of the stormy sea (Fig. 1), the wave-breaking events accompanied by the formation of spray and foam, are close to the crests of the dominant waves. Then, we suggest that the droplets are injected in the air flow near the wave crests and in the model, we explicitly take into account only the wave disturbances caused by the waves corresponding to the peak in the wind-wave spectrum.

Fig. 1 The panorama of water surface in the ocean under hurricane wind

The surface wave field was represented as the Stokes decomposition up to the third order. In the reference frame, following the wave, the surface elevation is

$$z_s = A\left(\cos kx^* + \frac{kA}{2}\cos 2kx^* + \frac{3(kA)^2}{8}\cos 3kx^*\right), \quad (19)$$

the horizontal velocity is

$$u_s = ckA\left(\left(1-\frac{1}{8}(kA)^2\right)e^{kz^*}\cos kx^* + \frac{kA}{2}e^{2kz^*}\cos 2kx^* + \frac{3kA}{8}e^{3kz^*}\cos 3kx^*\right), \quad (20)$$

and the vertical velocity

$$w_s = ckA\left(\left(1-\frac{1}{8}(kA)^2\right)e^{kz^*}\sin kx^* + \frac{kA}{2}e^{2kz^*}\sin 2kx^* + \frac{3kA}{8}e^{3kz^*}\sin 3kx^*\right). \quad (21)$$

The wave-induced perturbations of the air flow were calculated in the framework of the model of atmospheric boundary layer over the wavy water surface described in (Troitskaya and Reutov 1995; Troitskaya and Rybushkina 2008). In numerical modeling, they were approximated by the analytical formulas. The expression for the average horizontal air flow velocity is

$$U_0(z^*) = -u_{\text{spray}}(z^*) + \begin{cases} \dfrac{u_*}{\kappa}\dfrac{z^*}{z_0\gamma}\ln\gamma; & z^* < \gamma z_0, \\ \dfrac{u_*}{\kappa}\ln\dfrac{z^*}{z_0}; & z^* > \gamma z_0, \end{cases} \quad (22)$$

where $\gamma = 3$. For the wave-induced perturbations of the air velocity, we applied the following approximate expressions for the horizontal component:

$$U_1(z^*) = (U_0(z^*) + c)kA\left(e^{-kz^*}\cos kx^* + \frac{kA}{2}e^{-2kz^*}\cos 2kx^* + \frac{3kA}{8}e^{-3kz^*}\cos 3kx^*\right), \quad (23)$$

for the vertical component:

$$W_1(z^*) = (U_0(z^*) + c)kA\left(e^{-kz^*}\sin kx^* + \frac{kA}{2}e^{-2kz^*}\sin 2kx^* + \frac{3kA}{8}e^{-3kz^*}\sin 3kx^*\right), \quad (24)$$

which, as can be seen from Fig. 2, agree with the numerical results.

5 A model of spray generation

Spray contribution to the turbulent momentum flux depends on the initial velocities of the droplets leaving the water surface. These velocities define initial conditions for Eqs. (14) and (15) and depend on the mechanism of spray generation. Here, we consider the two principal mechanisms considered in the literature (Soloviev and Lukas 2014). It should be noticed that recently, a new mechanism of generation of droplets has been observed in laboratory conditions (Veron et al. 2012), but at the moment, it is not quantified and not considered here. According to the first mechanism (referred hereafter as Koga's mechanism), the Kelvin-Helmholtz instability on the air-water boundary leads to a development of small "projections" mainly on the crests of breaking waves, which stretch and then break to droplets (Koga 1981).

According to (Koga 1981), the speed of these droplets on a takeoff from the water surface varies from 0.5 to 2.5 of the phase velocity of the dominant wave. It should be noticed that very short fetch is typical for laboratory conditions and the phase velocities of waves are more than an order less than the wind speed. Thus, strongly nonlinear waves with many breaking events are observed. In the field conditions, wave breaking has been explored recently by Kleiss and Melville (2010), and Phillips function $\Lambda(c)$ has been obtained which is the velocity distribution function of the breaking wave crests' lengths (Fig. 3). It has been demonstrated that the breaking wave crests have velocities up to $10u_*$ with a pronounced peak at $5u_*$. By meaning of the phenomenon of wave breaking, initial velocities of the droplets leaving the crest should be equal to the crest velocity, and the number of the droplets—proportional to the length of the crest. On this basis, the distribution function of initial velocities of droplets was taken proportional

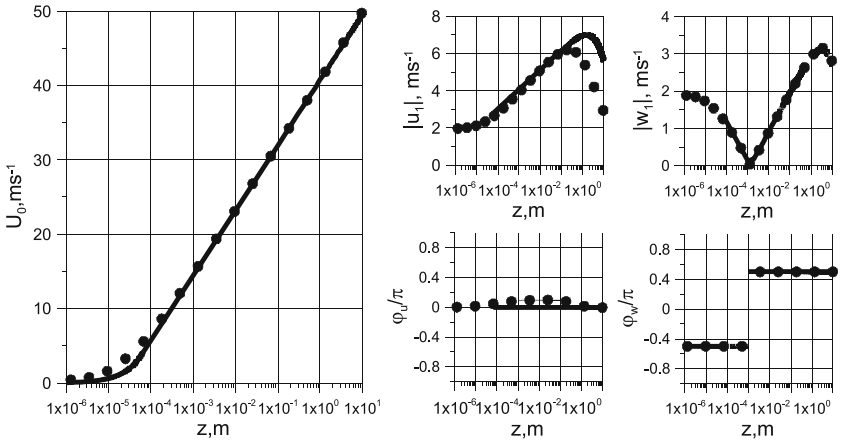

Fig. 2 The mean wind velocity profile and the wave-induced perturbations of the *vertical* and *horizontal* velocity components. *Filled circles* denote profiles, calculated in the framework of the model of turbulent boundary layer under the Boussinesq approximation, *solid curves* correspond to the formulas (22)–(24)

to $\Lambda(c)$. The angle distribution of initial droplets' velocities was supposed uniform within the range 0–45° to the horizontal.

Another mechanism of spray generation is connected with bursting of air bubbles on the water surface. When a bubble bursts, it produces a jet subsequently breaking into droplets due to the Rayleigh-Taylor instability. These droplets have velocities, depending on the bubble diameter (Blanchard 1963; Spiel 1994, 1997). The dependence of initial velocity of the droplet on its radius (Spiel 1995) can be approximated by the function

$$\begin{aligned} V_a &= v_0 \exp(-a/a_0) \quad ; \\ v_0 &= 8.4 \ \mathrm{ms}^{-1}; \ \ a_0 = 141.5 \ \ \mu\mathrm{m} \end{aligned} \tag{25}$$

According to the Koga's mechanism of spray generation, the initial conditions are as follows

$$x|_{t=0} = x_0; \quad z|_{t=0} = z_0(x_0); \quad u|_{t=0} = c; \quad w|_{t=0} = c \ \tan\theta; \tag{26}$$

where c is the random quantity with the density distribution function proportional to the Phillips function $\Lambda(c)$ taken from

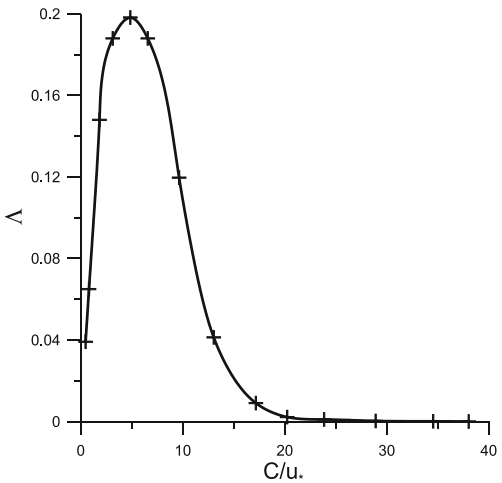

Fig. 3 Velocity distribution function of the lengths of breaking wave crests according to (Kleiss and Melville 2010)

(Kleiss and Melville 2010), θ is a random angle of injection within the uniform distribution between 0 and 45°. Here, we assume that at $t=0$ the droplet is on the water surface, i.e., its vertical z_0 and horizontal x_0 coordinates satisfy the expression for the water displacement in the Stokes wave (19). The amplitude of the wave A is determined by the wave age parameter $\Omega = \frac{U_{10}}{c_p}$ according to the empirical formula suggested by Donelan and Pierson (1987):

$$A = \frac{0.207}{2^{3/2}\Omega^{0.46}k_p}, \tag{27}$$

k_p and c_p are the wave number and phase velocity of the peak wave.

For the second mechanism (bubbles bursting), the initial conditions are

$$\begin{aligned} x|_{t=0} = x_0; \ \ z|_{t=0} = z_0(x_0); \ \ u|_{t=0} \\ = u(x_0, z_0) + v_x; \ \ w|_{t=0} = w(x_0, z_0) + v_y; \end{aligned} \tag{28}$$

where $v_x = V_a \cos\theta$, $v_y = V_a \sin\theta$, $0° < \theta < 180°$ and V_a is given by (25).

6 The statistics of droplets

The number of droplets, injected in atmospheric boundary layer from the sea surface, is described by the sea spray generation function $\frac{dF_0}{da}$ ($\frac{dF_0}{da}da$ gives the number of the droplets with the radii in the interval $[a, a+da]$ injected in the air flow from unit surface per unit time). Dimension of $\frac{dF_0}{da}$ is $(\mathrm{m}^2\ \mathrm{s}\ \mu\mathrm{m})^{-1}$, if the dimension of droplet radius is micrometers and of the surface area square meters.

The empirical sea spray generation function taking into account spume droplets was suggested by Andreas (1998).

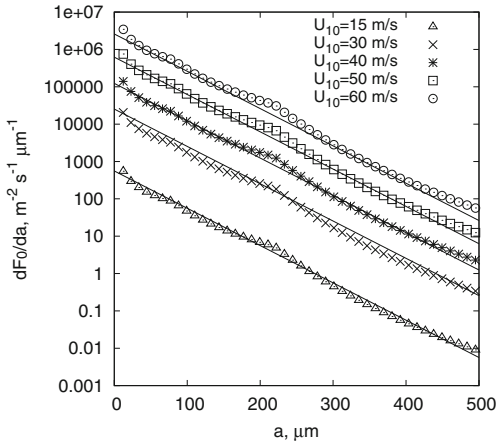

Fig. 4 The sea spray generation functions (Andreas 1998) for different wind speeds. *Solid curves* are the approximations by Eq. (31)

Figure 4 demonstrates the dependences $\frac{dF_0}{da}$ for different wind speeds from 15 to 60 m/s. The curves can be approximated by the exponential functions

$$\frac{dF_0}{da} = be^{-\chi a}, \tag{29}$$

where $\chi = 0.023\ \mu m^{-1} = 230\ cm^{-1}$, and b is a function of wind speed, which can be approximated by the polynomial:

$$b = b_0 (U_{10}/u_0)^d, \tag{30}$$

with $b_0 = 1.9 \cdot 10^{-4}\ (m^2\ s\ \mu m)^{-1} = 1.9 \cdot 10^{-4}\ (cm^3\ s)^{-1}$, $u_0 = 1$ m/s, $d = 5.5$ for $U_{10} < 40$ m/s (we used $d = 5.6$ for $U_{10} = 50$ m/s and $d = 5.7$ for $U_{10} = 60$ m/s). Finally, we obtain:

$$\frac{dF_0}{da} = b_0 \left(\frac{U_{10}}{u_0}\right)^d e^{-\chi a}. \tag{31}$$

Equation (31) has higher power dependence of the generation function on the wind speed than in (Andreas 1998). Possibly, this is due to the small droplets ($a < 20$ μm) originated from the bubble bursts. However, these droplets do not contribute significantly to the momentum flux (see estimates by Kudryavtsev and Makin (2011)) and they are neglected here.

In order to calculate the momentum, delivered by the wind to spray in the layer over the distance z^* from the water surface, i.e., the function $F(z^*)$ in Eq. (10), it is necessary to calculate the horizontal momentum gained by the droplet of the radius a when it moves above z^*. Note that for $z^* = 0$, it corresponds to the total momentum of the droplet gained during its life cycle from being injected from the water surface to falling down to water.

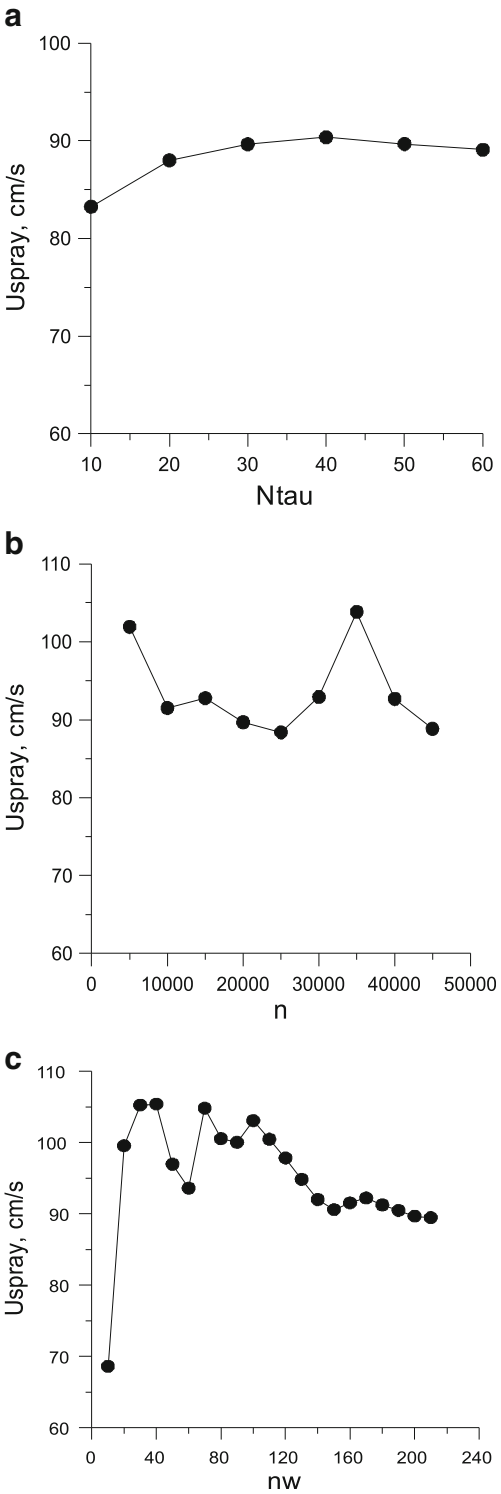

Fig. 5 Tests: u_{spray} as the function of the time step (**a**), u_{spray} as the function of the number of time steps (**b**), and u_{spray} as the function of the number of the realizations of Markovian process (**c**) for $U_{10} = 40$ m/s, $\Omega = 3$

Averaging over N realizations of the Markovian process (i.e., turbulent fluctuations in the atmosphere), over the angles and taking into account Eq. (31), we obtain:

$$F(z^*) = \frac{1}{\theta_t}\int_{a_{\min}}^{a_{\max}} \frac{dF_0}{da} da \int_0^{\theta_t} d\theta \frac{1}{N}\sum_{n=1}^{N} p_{nx}(a, u_*, z^*, \theta). \quad (32)$$

7 Results of the numerical experiments and discussion

Before the calculations, we defined the maximum time step Δt and minimal statistical ensemble providing statistical convergence of the problem. As a criterion of convergence, we used the time dependence of the value

$$u_{\text{spray}} = \int_0^{\infty} \frac{F(z')/\rho_a}{K_m(z')} dz'. \quad (33)$$

The integration time step Δt was selected variable and equal to the minimum between time scales $\tau_w^p / N_{\text{tau}}$ and $(T_R/K) / N_{\text{tau}}$, which kept it small compared to both of the characteristic time scales in Eq. (14) and (15). The dependence of u_{spray} on N_{tau} is shown in Fig. 5a; it approaches the constant value for $N_{\text{tau}} > 20$. We investigated the dependence of u_{spray} on the number of time steps n and the number of realizations of Markovian process nw. The results are shown in Fig. 5b, c. Based on the tests $N_{\text{tau}} = 20$, $n = 20{,}000$, and $nw = 200$ were chosen for calculations.

Figure 6 shows trajectories of droplets of different sizes in the turbulent boundary layer over the wavy water surface, for which the initial conditions were specified by the Koga's mechanism. It can be seen that a significant number of droplets injected from the water surface fall down to water. Dependences of the horizontal velocities of the droplets on time shown in the right panels characterize the intensity of momentum exchange between the droplets and the air flow. As follows from Fig. 6, the largest changes are experienced by the droplets that become levitating. These droplets are accelerated from their initial velocities to the local wind speed and thus take the momentum from the air flow. The droplet falling back to the water may have velocity either larger or smaller than initial velocity; however, the total change of their velocities is small compared to the wind speed on the standard height.

Within both mechanisms, we calculated the dependencies of the momentum p, gained by the droplets during their life cycle, on radii of droplets (Figs. 7 and 8).

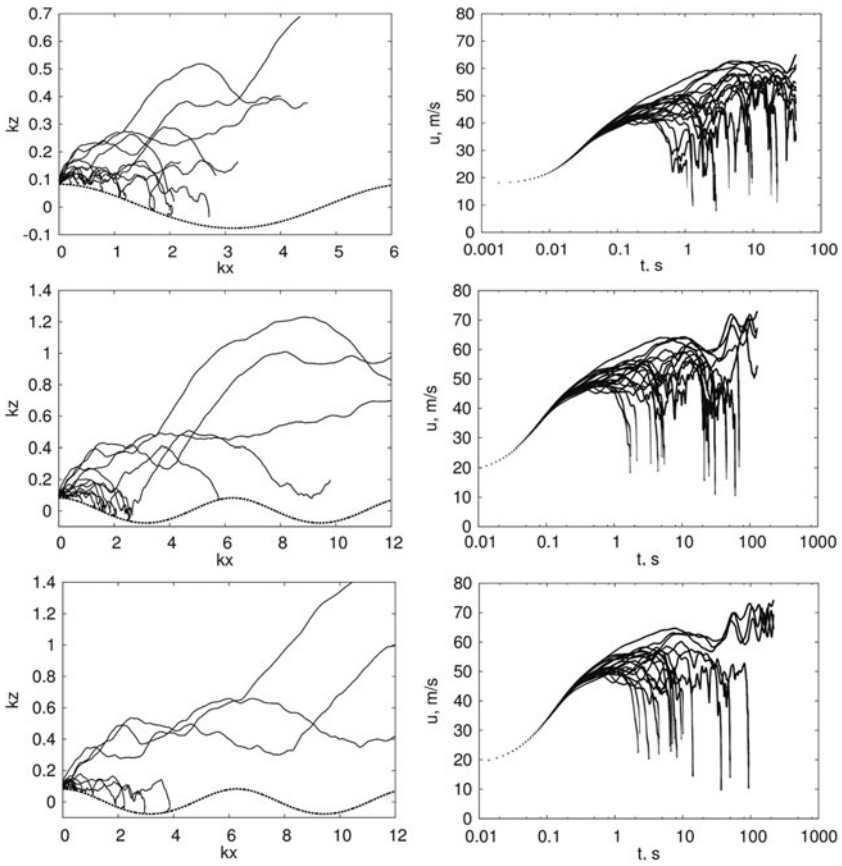

Fig. 6 Trajectories of the droplets in the turbulent air flow (*on the left*) and their horizontal velocities as the functions of time (*on the right*) for $U_{10} = 50$ m/s, $\Omega = 1.2$. The radii of droplets are $a = 50$ μm (*upper figures*), $a = 100$ μm (*middle figures*), $a = 150$ μm (*lower figures*)

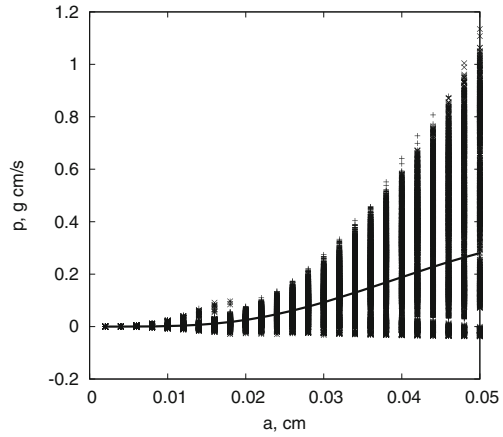

Fig. 7 Momentum gained by each droplet in the air flow for Koga's model of spray generation mechanism ($U_{10}=50$ m/s, $\Omega=1.2$). *Solid curve* corresponds to the average value

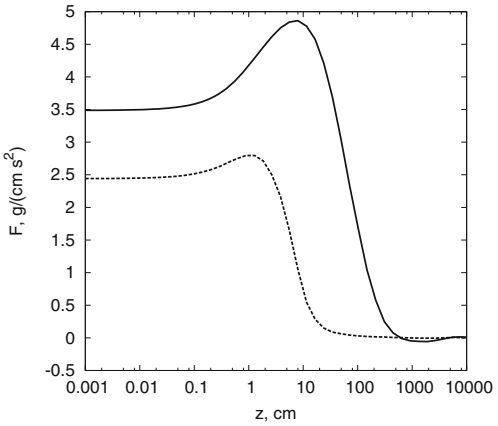

Fig. 9 Function $F(z)$: *solid curve* Koga's mechanism of spray generation, *dashed curve* the mechanism of bubbles bursting ($U_{10}=50$ m/s, $\Omega=1.2$)

For Koga's mechanism of sea spray generation, droplets are larger and they have larger velocities. Thus, the momentum exchange is more effective for the first mechanism which is seen from comparing Figs. 7 and 8. Note that there are a number of droplets delivering momentum to the air flow during their life cycles. This effect is more pronounced for the large droplets ($a>200$ μm). However, the average momentum gained by all the droplets of the same size is positive. This leads to the negative additive to the wind speed and to an increase in the drag due to the effect of spray.

Figure 9 shows the functions $F(z^*)$ characterizing the momentum delivered by the air flow to spray in the layer over z^* for the two models of sea spray injection. Employing $F(z^*)$, we can calculate the contribution to the sea surface drag from the spray momentum exchange with the air flow. The dependences of the drag coefficient on the wind speed (Fig. 10) demonstrate that the air-spray momentum exchange leads to the increase of the drag (for the mechanisms of sea spray generation that are known at present). When spray is not taken into account, the drag coefficient saturates at strong winds. The account of spray leads to increase in the drag coefficient, up to 30–40 % at $U_{10}=60$ m/s. The drag coefficient calculated in the framework of our model is consistent with the available experimental data from Bell et al. (2012), French et al. (2007), and Vickery et al. (2009).

It should be noted, however, that more strictly, according to Holthuijsen et al. (2012), surface drag depends significantly on the sector of the tropical cyclone, where it is measured. They present the experimental data for the tropical cyclone sorted over the azimuthal sectors, or equivalently, the type of swell: left-front sector (cross swell), right-front sector (following swell) and rear (opposing swell). Strictly speaking, the formulation of the problem, considered in the present work, corresponds to the conditions in the right-front sector of the tropical cyclone, where waves propagate in the direction along the wind. According to Holthuijsen et al. (2012), in this sector, the weak increase of the aerodynamic drag coefficient is observed for the wind speeds exceeding 40 m/s (Fig. 11). Our calculations in the framework of the present model agree with the data of measurements.

We have demonstrated that the effect of air-spray momentum exchange for the known mechanisms of spray generation leads to the deceleration of the wind flow and increase in the

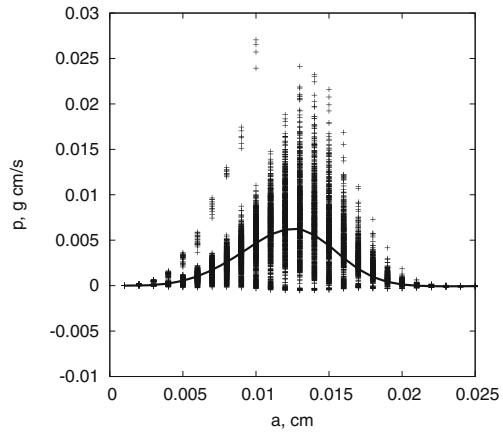

Fig. 8 As in Fig. 7 for the mechanism of bubbles bursting ($U_{10}=50$ m/s, $\Omega=1.2$)

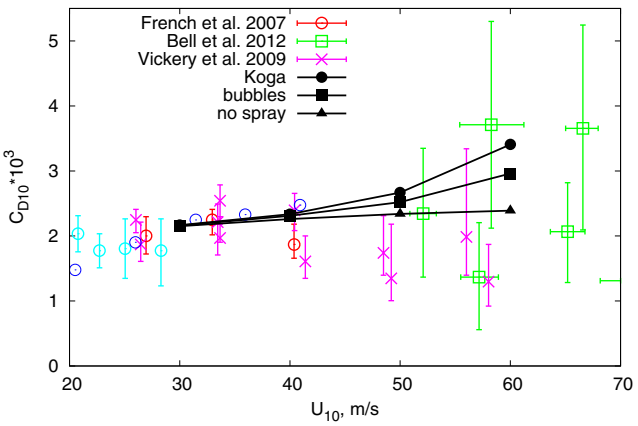

Fig. 10 Drag coefficient for the two mechanisms of the sea spray generation compared to the data of the field experiments

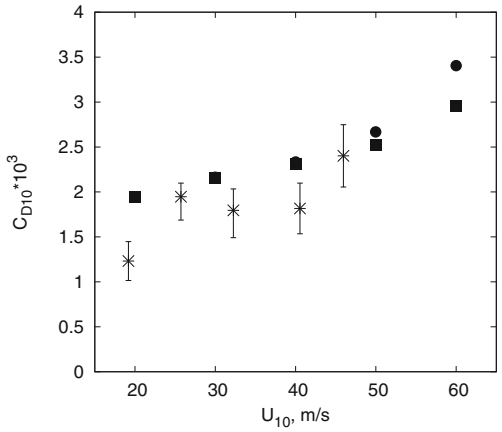

Fig. 11 Drag coefficient for the two mechanisms of the sea spray generation and the experimental data measured in the right sector of the tropical cyclone (Holthuijsen et al. 2012)

drag coefficient. Note that, here, we have not accounted for the stratification created by suspended droplets in the air (Bye and Jenkins 2006; Bye et al. 2010, 2014), which can be done independently basing on the Monin-Obukhov similarity theory as it is explained by Bye and Jenkins (2006) and Bao et al. (2011). We can expect that it will lead to the decrease of the surface drag, but the quantitative effect is significantly uncertain due to strong uncertainty of the spray generating function especially at strong winds (Veron 2015).

8 Conclusions

A stochastic model of the life cycle of the droplet injected from the sea surface to the air is developed. The interaction of droplets with the air flow is modeled in terms of the Markovian chain. The interaction model consists of the model of motion of heavy particle in the forcing air flow, the model of the wind flow, the model of spray generation, and the statistics of droplets. Two mechanisms of the spray generation are considered: first, droplets are injected into the air with the velocities of the breaking wave crests (Koga's mechanism); second, they appear from the collapsing buoyant bubbles on the water surface. Calculations within the model demonstrate that a droplet may either deliver or gain the momentum during its life cycle depending on peculiarities of the air velocity field, wave parameters, and the droplet's radius, with the overall effect that the sea spray decelerates the air flow and increases the drag.

We admit that our results depend on the assumptions within the model. The most uncertain elements of the model are the mechanism of the sea spray generation, defining the initial velocities of droplets on the takeoff from the surface, and the spray statistics, based on the field measurements of the spray concentration (Veron 2015 and references therein). To specify these parameters, special experimental investigations employing modern experimental techniques are required. As for now, our basic result is that the sea spray leads to increase in the surface drag instead of its generally assumed decrease on the assumption that the velocity profile is neutral. Hence, one can expect that the stratification produced by the presence of spray balances this growth and gives leveling or peaking surface drag at extremely high winds.

Acknowledgments This work was supported by the grant of the government of the Russian Federation (contract 11.G34.31.0048); the European Commission ERC-Ideas PoC Project 632295-INMOST (2014–2015); the Academy of Finland project 'Atmosphere-hydrosphere interaction in the Baltic Basin and Arctic Seas' ABBA Contract No. 280700 (2014–2017); RFBR (nos. 16-05-00839, 14-05-91767). Numerical code development and numerical modeling were supported by the Russian Science Foundation (nos. 14-17-00667 and 15-17-20009, respectively). YT was partially supported by FP7 collaborative Project No. 612610. Insightful comments by the referees are gratefully acknowledged.

Appendix. Derivation of the law of the momentum flux conservation

Here, we derive the conservation law for the momentum flux averaged over horizontal coordinate. Transforming Eq. (5) with account of Eq. (6) in Section 1 gives:

$$\frac{\partial \rho_a \langle u\rangle}{\partial t^*}+\frac{\partial}{\partial z^*}\left(\rho_a\langle u\rangle\left(\langle v\rangle-\frac{\partial \eta}{\partial t^*}-\langle u\rangle\frac{\partial \eta}{\partial x^*}\right)\right)+\frac{\partial \rho_a\langle u\rangle^2}{\partial x^*}+ +\frac{\partial\langle p\rangle-\rho_a\sigma_{xx}}{\partial x^*}-\frac{\partial}{\partial z^*}\left((\langle p\rangle-\rho_a\sigma_{xx})\frac{\partial \eta}{\partial x^*}\right)=\frac{\partial \rho_a\sigma_{xz}}{\partial z^*}+f. \tag{A1}$$

Averaging (A1) over the coordinate x^* yields the conservation law for the momentum flux in MABL in curvilinear coordinates:

$$\frac{\partial \rho_a \overline{\langle u\rangle}^{x^*}}{\partial t^*}+\frac{\partial}{\partial z^*}\left(\overline{\rho_a\langle u\rangle\left(\langle v\rangle-\frac{\partial \eta}{\partial t^*}-\langle u\rangle\frac{\partial \eta}{\partial x^*}\right)}^{x^*}-\overline{(\langle p\rangle-\rho_a\sigma_{xx})\frac{\partial \eta}{\partial x^*}}^{x^*}\right) =\frac{\partial \rho_a\overline{\sigma_{xz}}^{x^*}}{\partial z^*}+\overline{f}^{x^*}. \tag{A2}$$

In stationary conditions (A1) yields:

$$\frac{d}{dz^*}\left(\overline{\rho_a\langle u\rangle\left(\langle v\rangle-\frac{\partial \eta}{\partial t^*}-\langle u\rangle\frac{\partial \eta}{\partial x^*}\right)-(\langle p\rangle-\rho_a\sigma_{xx})\frac{\partial \eta}{\partial x^*}}^{x^*}\right) =\frac{d\rho_a\overline{\sigma_{xz}}^{x^*}}{dz^*}+\overline{f}^{x^*}. \tag{A3}$$

Integrating (A3) over z^* and taking into account the boundary condition $\sigma_{xz}^{\overline{\quad x^*}} \to u_*^2$ when $z^* \to \infty$, yields the following expression for the conservation of momentum flux:

$$\rho_a \overline{\sigma_{xz}}^{x^*} = \rho_a u_*^2 - \rho_a \tau_{\mathrm{wave}}(z^*) - F(z^*). \tag{A4}$$

Here

$$\tau_{\mathrm{wave}}(z^*) = -\overline{\langle u\rangle \left(\langle v\rangle - \frac{\partial \eta}{\partial t^*} - \langle u\rangle \frac{\partial \eta}{\partial x^*}\right) + \left(\frac{\langle p\rangle}{\rho_a} - \sigma_{xx}\right)\frac{\partial \eta}{\partial x^*}}^{x^*} \tag{A5}$$

is a wave momentum flux caused by the form drag of the water surface (a function of z^* decreasing with the distance from the surface).

$$F(z^*) = -\int_{z^*}^{\infty} \bar{f}^{x^*}(z')dz' \tag{A6}$$

is the momentum delivered from the air flow to spray in the layer from current z^* to infinity.

References

Andreas EL (1998) A new sea spray generation function for wind speeds up to 32 m s^{-1}. J Phys Oceanogr 28:2175–2184

Andreas EL (2004) Spray stress revised. J Phys Oceanogr 34:1429–1440

Andreas EL, DeCosmo J (1999) Sea spray production and influence on air-sea heat and moisture fluxes over the open ocean. In: Geernaert GL (ed) Air-sea exchange: physics, chemistry and dynamics. Kluwer Academic Publishers, Dordrecht, pp 327–362

Andreas EL, Edson JB, Monahan EC, Rouault MP, Smith SD (1995) The spray contribution to net evaporation from the sea. Bound Lay Meteorol 72:3–52

Andreas EL, Mahrt L, Vickers D (2012) A new drag relation for aerodynamically rough flow over the ocean. J Atmos Sci 69:2520–2536

Bao J-W, Fairall CW, Michelson SA, Bianco L (2011) Parameterizations of sea-spray impact on the air–sea momentum and heat fluxes. Mon Weather Rev 139:3781–3797

Bell M, Montgomery MT, Emanuel KA (2012) Air-sea enthalpy and momentum exchange at major hurricane wind speeds observed during CBLAST. J Atmos Sci 69:3197–3222

Blanchard DC (1963) The electrification of atmosphere by particles from bubbles in the sea. Prog Oceanogr 1:171–202

Bye JAT, Jenkins AD (2006) Drag coefficient reduction at very high wind speeds. J Geophys Res 111:C03024. doi:10.1029/2005JC003114

Bye JAT, Ghantous M, Wolff J-O (2010) On the variability of the Charnock constant and the functional dependence of the drag coefficient on wind speed. Ocean Dyn 60:851–860

Bye JAT, Wolff J-O, Lettmann KA (2014) On the variability of the Charnock constant and the functional dependence of the drag coefficient on wind speed: part II—observations. Ocean Dyn 64:969–974

Donelan MA, Pierson WJ (1987) Radar scattering and equilibrium ranges in wind-generated waves—with application to scatterometry. J Geophys Res 92:4971–5029

Donelan MA, Haus BK, Reul N, Plant WJ, Stiassnie M, Graber HC, Brown OB, Saltzman ES (2004) On the limiting aerodynamic roughness of the ocean in very strong winds. Geophys Res Lett 31:L18306

Edson JB, Fairall CW (1994) Spray droplet modeling. 1. Lagrangian model simulation of the turbulent transport of evaporating droplets. J Geophys Res 99(C12):25295–25311

Foreman RJ, Emeis S (2010) Revisiting the definition of the drag coefficient in the marine atmospheric boundary layer. J Phys Oceanogr 40:2325–2332

French JR, Drennan WM, Zhang JA, Black PG (2007) Turbulent fluxes in the hurricane boundary layer. J Atmos Sci 64:1089–1102

Holthuijsen LH, Powell MD, Pietrzak JD (2012) Wind and waves in extreme hurricanes. J Geophys Res 117:C09003. doi:10.1029/2012JC007983

Jarosz E, Mitchell DA, Wang DW, Teague WJ (2007) Bottom-up determination of air-sea momentum exchange under a major tropical cyclone. Science 315:1707–1709

Kleiss JM, Melville WK (2010) Observations of wave breaking kinematics in fetch-limited seas. J Phys Oceanogr 40:2575–2604

Koga M (1981) Direct production of droplets from breaking wind-waves—its observation by a multi-colored overlapping exposure photographing technique. Tellus 33:552–563

Kudryavtsev VN (2006) On the effect of sea drops on the atmospheric boundary layer. J Geophys Res 111:C07020

Kudryavtsev VN, Makin VK (2007) Aerodynamic roughness of the sea surface at high winds. Bound Lay Meteorol 125(2):289–303

Kudryavtsev V, Makin V (2011) Impact of ocean spray on the dynamics of the marine atmospheric boundary layer. Bound Lay Meteorol 40(3):383–410

Makin VK (2005) A note on drag of the sea surface at hurricane winds. Bound Lay Meteorol 115(1):169–176

Powell MD, Vickery PJ, Reinhold TA (2003) Reduced drag coefficient for high wind speeds in tropical cyclones. Nature 422:279–283

Smol'yakov AV (1973) Quadrupole radiation spectrum of plane turbulent boundary layer. Sov Phys Acoust 19:271–276

Soloviev A, Lukas R (2014) The near-surface layer of the ocean: structure, dynamics, and applications, 2nd edn. Springer Science + Business Media, Dordrecht

Spiel DE (1994) The sizes of the jet droplets produced by air bubbles bursting on sea- and fresh-water surfaces. Tellus 46B:325–338

Spiel DE (1995) On the birth of jet drops from bubbles bursting on water surfaces. J Geophys Res 100:4995–5006

Spiel DE (1997) More on the births of jet drops from bubbles bursting on seawater surfaces. J Geophys Res 102:5815–5821

Troitskaya YI, Reutov VP (1995) Nonlinear growth rate of wind water waves and their excitation near the stability threshold. Radiophys Quantum Electron 38(3-4):133–136

Troitskaya YI, Rybushkina GV (2008) Quasi-linear model of interaction of surface waves with strong and hurricane winds. Izv Atmos Oceanic Phys 44(5):621–645

Troitskaya Y, Sergeev D, Kandaurov A, Kazakov V (2011) Air-sea interaction under hurricane wind conditions. In: Lupo A (ed.) Recent hurricane research—climate, dynamics and social impacts, InTech, Rijeka, Croatia, pp 247–268

Troitskaya YI, Sergeev DA, Kandaurov AA, Baidakov GA, Vdovin MA, Kazakov VI (2012) Laboratory and theoretical modeling of air-sea momentum transfer under severe wind conditions. J Geophys Res 117:C00J21

Veron F (2015) Ocean spray. Annu Rev Fluid Mech 39:419–446

Veron F, Hopkins C, Harrison EL, Mueller JA (2012) Sea spray spume droplet production in high wind speeds. Geophys Res Lett 39:L16602

Vickery PJ, Wadhera D, Powell MD, Chen Y (2009) A hurricane boundary layer and wind field model for use in engineering applications. J Appl Meteorol Climatol 48:381–405